Seeing Through the Skull: Advanced EEGs Use MRIs to Accurately Measure Cortical Activity from the Scalp

Alan Gevins, Jian Le, Paul Brickett, Bryan Reutter, and John Desmond

Summary: There is a vast amount of untapped spatial information in scalp- recorded EEGs. Measuring this information requires use of many electrodes and application of spatial signal enhancing procedures to reduce blur distortion due to transmission through the skull and other tissues. Recordings with 124 electrodes are now routinely made, and spatial signal enhancing techniques have been developed. The most advanced of these techniques uses information from a subject's MRI to correct blur distortion, in effect providing a measure of the actual cortical potential distribution. Examples of these procedures are presented, including a validation from subdural recordings in an epileptic patient. Examples of equivalent dipole modeling of the somatosensory evoked potential are also presented in which two adjacent fingers are clearly separated. These results demonstrate that EEGs can provide images of superficial cortical electrical activity with spatial detail approaching that of O15 PET scans. Additionally, equivalent dipole modeling with EEGs appears to have the same degree of spatial resolution as that reported for MEGs. Considering that EEG technology costs ten to fifty times less than other brain imaging modalities, that it is completely harmless, and that recordings can be made in naturalistic settings for extended periods of time, a greater investment in advancing EEG technology seems very desirable.

Key words: High-resolution EEG; Evoked potential; MRI; Spatial signal enhancement; Deblurring; Finite element model; Laplacian derivation.

Introduction

Although the EEG has been measured for over 60 years, and the averaged evoked potential for over 30, their full potential as brain imaging technologies has not yet been realized. This is not due to an inherent lack of information in EEGs, but to a relative lack of commitment of resources to get at it. The quantity and quality of information obtainable from EEGs is currently limited by the number of scalp recording sites and the amount and type of numerical computing applied. Since the former is only a matter of habit, and since computing has become so powerful and inexpensive, we feel that it is now timely for the imaging capability of EEGs to make a major advance.

Much of the groundwork for this development has already been accomplished, including recording from more than 100 sites for improved spatial sampling (Gevins et al. 1990), precise measurement and registration of electrode positions with 3-D MRI images (Gevins 1989), means for reducing the spatial blur distortion which occurs when potentials are conducted through the skull (Gevins 1989; Gevins et al. 1990; Le and Gevins In Prep. a,b), computation of the "center of mass" of cortical areas activated by sensory stimulation (equivalent dipoles; Fender 1987), extraction of spatial multivariate features and classification of spatial brain states using neural-network pattern recognition techniques (Gevins 1980; Gevins and Morgan 1988), split-second measures of functional cortical networks (Gevins et al. 1981, 1989), development of quantitative norms for clinical studies (John 1977), and a myriad of other technical developments (reviews in Lopes da Silva et al. 1986; Duffy 1986; Gevins and Remond 1987; Basar 1988; Pfurtscheller and Lopes da Silva 1988; also see special issues of Brain Topography, 1989, Vol. 2(1/2), and 1990 Vol 3(1)). Although a considerable effort has already been made in many of these areas, an additional major effort will be required to further refine, integrate and validate EEG spatial enhancement methods, and then to disseminate technologies embodying them.

In considering whether it is worth further developing and modernizing the EEG, it is relevant to note that every

EEG Systems Laboratory and Sam Technology, San Francisco CA, USA.

Accepted for publication: September 23, 1991.

Supported by the National Institute of Neurological Diseases and Stroke, the National Institute of Mental Health, the National Institute of Health, the Air Force Office of Scientific Research, the Air Force School of Aerospace Medicine and the Office of Naval Research. Access to neurosurgery patients was kindly provided by the Northern California Comprehensive Epilepsy Center at the University of California (San Francisco), Dr. Kenneth Laxer, Director, and Dr. Nicolas Barbaro, Neurosurgeon. Contributions to the research presented here were also made by our colleagues at EEG Systems Laboratory including Jim Alexander, Brian Cutillo, Judy McLaughlin, and Michael Ward.

Correspondence and reprint requests should be addressed to Alan Gevins, EEG Systems Laboratory, 51 Federal, San Francisco, CA, 94017, USA.

brain imaging modality has its relative strengths and limitations in terms of spatial and temporal resolution, the nature of the processes measured, and economic and logistical factors. For example, while O15 PET is one of the imaging methods with the best spatial resolution, which is approximately 6 to 100 mm for modern PET machines (full width at half maximum; M. Raichle, personal communication; Mintun et al. 1989), O15 PET also has a number of disadvantages which are not often considered: 1) the required time sample of 45-60 seconds is far too long to measure split-second neural processes of seizure generation or of cognition; 2) the experimental designs for PET are highly restricted by safety limitations on allowable dosages of ionizing radiation; and 3) it costs roughly five million dollars for a PET facility. While not comparable to PET in 3-D resolution of many simultaneously active areas throughout the neuroaxis, we believe that improved EEG measures can provide images of superficial cortical activity with a spatial resolution of 1-2 square centimeters, and an unsurpassed millisecond-range temporal resolution. Low cost (in the one hundred to two hundred thousand dollar range), complete harmlessness, ability to record for extended periods of time in a comfortable setting, and opportunity to record the same subject many times make EEG measures additionally attractive.

124-Channel EEG Recordings

Until recently it was assumed by most researchers that, due to the smearing effects of volume conduction, the 19 electrodes of the basic 10-20 system were sufficient for sampling the spatial information of EEG or EP signals at the scalp. This is clearly not the case, as has been amply demonstrated (Lehmann 1986; Wang et al. 1989; Gevins 1989, 1990). Figure 1 is an example which shows that the EEG as normally recorded is spatially undersampled. Isopotential maps are drawn on a scalp surface reconstructed from horizontal MR images of that subject. Data shown are somatosensory evoked potentials to 15-Hz stimulation of the left middle and right index fingers, for a maximum of 122 channels and desampled to 57, 31 and 18 channels. The spline interpolation algorithm makes all the maps visually appealing, but only in the 122-channel version is the presence of two separate peaks obvious, corresponding to the two fingers stimulated.

With the original nineteen electrodes of the 10-20 System (Jasper 1958), the typical distance between electrodes on an average adult male head is about 6 cm; with 124 electrodes, the typical distance is 2.25 cm. This is a good improvement in sampling resolution, but further improvements are possible since the 3 dB point of the point spread function for conductance of potentials from the brain surface to the scalp averages about 2.5 cm (Gevins 1990). Thus, additional information could be obtained by recording with more electrodes spaced closer together, and then applying signal enhancing methods such as those described below to extract more independent information from each electrode. A good goal for future development is 256 channels which provides an inter-electrode distance of about 1.6 cm.

Previous papers have described our traditional methods for recording EEGs from 124 scalp sites and measuring the three-dimensional position of each electrode (Gevins 1989; Gevins et al. 1990). Advanced systems for very rapid electrode placement and position measurement are currently being refined and tested in our laboratory. The two previous papers have also described our fifth generation EEG analysis software system which is a UNIX-based, network-distributed system written in the C language. A sixth generation system is currently under development in the C++ language. It is also a network-distributed system under UNIX, but it is based on the X-11 network windowing standard and incorporates an object-oriented database technology which will facilitate processing, viewing and retrieving multichannel time series and three-dimensional image data.

MRI Analysis and Modeling Methods

Our approach to 3-D anatomical modeling and visualization has been guided by our need to integrate anatomical data obtained from MRIs with functional data obtained from scalp and cortical EEGs. Although there are now several commercial visualization software packages which can generate 3-D perspective pictures from MRIs, we had to develop our own contouring and surface-based reconstruction techniques and associated MR processing and display methods as we are more concerned with 3-D mathematical modeling of the anatomical structures in the data than with visualization per se. By contrast, the commercial packages are concerned primarily with volume rendering (Levoy 1988; Levin et al. 1989) or surface modeling for visualization using discontiguous "ribbons" (Heffernan and Robb 1985; Jack et al. 1990; implemented by the Analyze software package of the Mayo Foundation) or unstructured lists of triangles created by the "marching cubes" algorithm (Lorensen and Cline 1987; implemented in the apE software package of the Ohio Supercomputer Center).

We developed methods and software to do automated threshold-based 2-D contouring of individual MR images, with optional manual editing, followed by the construction of triangular 3-D surface elements between contours in adjacent images. Our MR images have picture elements (pixels) with dimensions that are roughly 1 mm by 1 mm, and typically the image planes are separated from one another by 3 mm. Renderings of these surface models are created by using standard 3-D computer graphics techniques (Foley et al. 1990). For example, the surface is "illuminated" by a combination of direct light, skylight, and diffuse light, and the amount of light reflected from the surface to an arbitrary viewpoint is calculated. In addition to generating these realistic surface renderings, we are able to display data such as EPs or event-related covariances (a measure of functional networks — Gevins and Bressler 1988) on these surfaces. This results in powerful images that help to convey the 3-D complexity of anatomical structure and function. Previous papers have described our EEG-MRI alignment procedures (figure 2), as well as our basic MRI image analysis, recognition and visualization methods (Gevins et al. 1990; Reutter and Gevins In Prep.).

EEG Spatial Enhancement Methods

Electrical currents generated by sources in the brain are volume conducted through brain, CSF, skull and scalp to the recording electrodes. Because of this, potentials due to a localized source are spread over a considerable area of scalp and the potential measured at a scalp site represents the summation of signals from many sources over much of the brain. We have developed two spatial enhancement methods to correct this blur distortion; neither method requires specification of an arbitrary source model (e.g., current dipoles).

The simpler method computes a very accurate estimate of the surface Laplacian Derivation (LD), which is proportional to local normal current at the scalp. This has the advantage of eliminating the effect of the reference electrode used for recording, and of eliminating much of the common activity due to either the reference electrode or volume conduction from distant sources. The disadvantages are that the LD does not produce valid values at the outermost ring of electrodes and it does not correct for local differences in skull thickness and conduction properties. Although computing the LD at first seems trivial (Hjorth 1975), there are in fact a number of subtleties (Nunez 1989). The most accurate surface LD, which we have implemented, uses the actual measured electrode positions, and estimates the LD over the actual shape of the head using a 3-D spline algorithm (Le and Gevins In Prep. a). Figure 3 shows the LD for the same data as in figure 1 (lower right). A dramatic increase in spatial detail is apparent with the LD as compared with the linked-ear-reference.

A further improvement in distortion reduction is possible, in principle, by using a finite element model of the cortex, CSF, skull and scalp to estimate the potentials which would actually be recorded on the surface of the brain. We call our implementation of this method Finite Element Model Deblurring (FEMDB) (Gevins et al. 1990; Le and Gevins In Prep. b). The price of the improvement offered by FEMDB is that MRIs have to be recorded and processed and many more calculations have to be performed. Unlike other methods which estimate cortical potentials or currents (Nicholas and Deloche 1975; Freeman 1980; Hill et al. 1988; Sidman et al. 1989), FEMDB is a true "downward continuation" method in that, without prior knowledge or assumptions about the generating sources, the cortical potential distribution is derived given the scalp potential distribution and a realistic model of the conducting volume between the scalp and cortical surfaces. In the FEMDB, a transformation matrix is constructed based on the geometry and conductivities of the finite elements which predicts the scalp potentials for any given set of cortical potentials. Then an efficient iterative process is used to find the cortical potentials which result in the closest fit between this forward solution and the recorded data. Simulations of the method in a three sphere model showed that the estimated deblurring results are the same as an analytical computation of the exact solution (Le and Gevins In Prep. b). Experiments in which the skull conductivity constant was varied over a 50% range showed smooth and well-behaved effects on FEMDB (Le and Gevins In Prep. b).

Comparison of FEM Deblurring With Subdural Grid Recording

Initial results of FEMDB (figure 4) demonstrate an improvement in detail over the Laplacian Derivation (figure 5) and good agreement between the computed and the actual cortical evoked potentials (figure 6) (Le and Gevins In Prep. b). The data are from a patient with pharmacologically-intractable seizures for whom we have both scalp and subdural grid recordings of the steady-state somatosensory EP elicited by 15-Hz electrical stimulation of the right hand.

Examples of FEM Deblurring

An example is shown of deblurring for a normal male subject who was stimulated with 15 Hz auditory, visual and somatosensory stimuli. Figure 7 shows the deblurred steady-state evoked potentials for stimulation of each of three fingers. Responses to the left and right fingers are appropriately lateralized, and there is an obvious difference between the middle and index finger of the right hand. Figure 8 shows the 15 Hz auditory evoked potential, as well as the visual response to stimulation of the lower left and right visual quadrants.

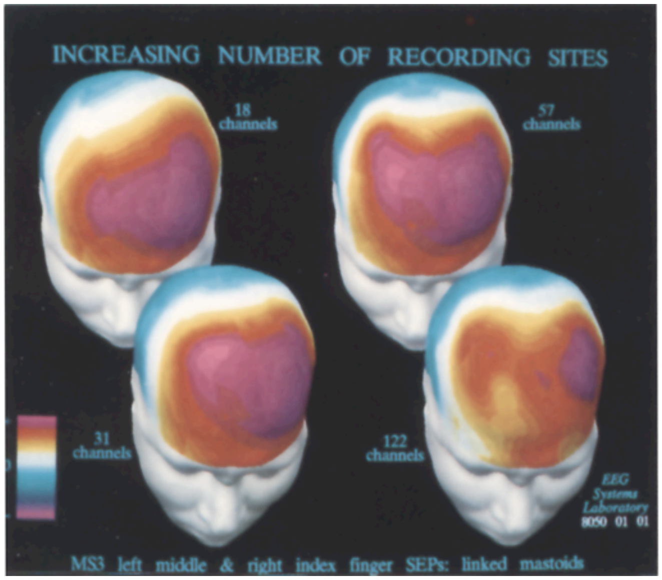

Figure 1. Steady-state somatosensory evoked potentials elicited by 15-Hz stimulation of left middle and right index finger are shown for an increasing number of channels from 18 to 122. The potential distributions are shown mapped on a reconstructed scalp surface made from that subject's MR images. Only the version with 122 channels shows the true topography, and allows clear visual identification of both the left and right-sided peaks.

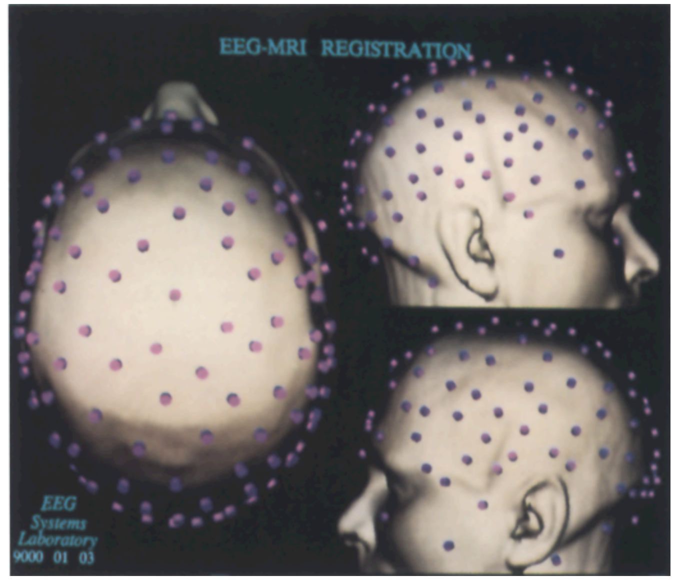

Figure 2. Electrodes are schematically displayed as small purple cylinders, at the actual measured positions, on a 3-D model of the subject's head constructed from his MR images.

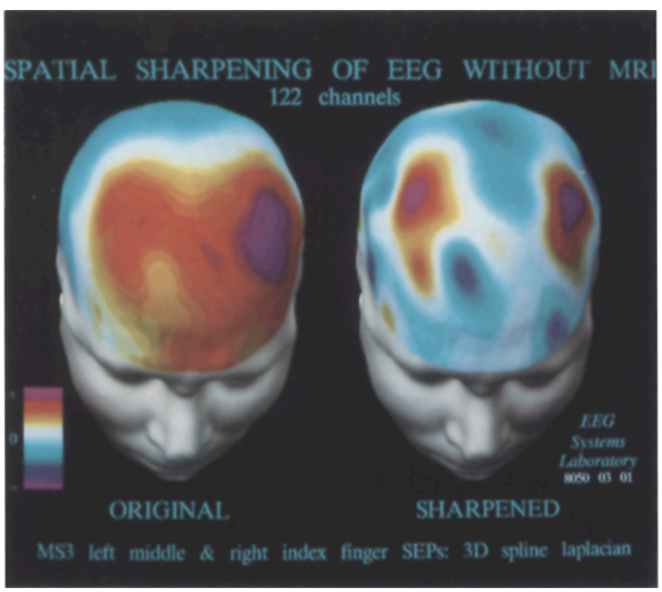

Figure 3. Potentials referenced to digitally linked ears (left — same data as figure 1, lower right) and 3-D spline Laplacian Derivation (right) compared for 122-channel, steady-state somatosensory evoked potentials elicited by stimulation of left middle and right index fingers. The Laplacian Derivation clearly isolates peaks that were merged together in the potentials.

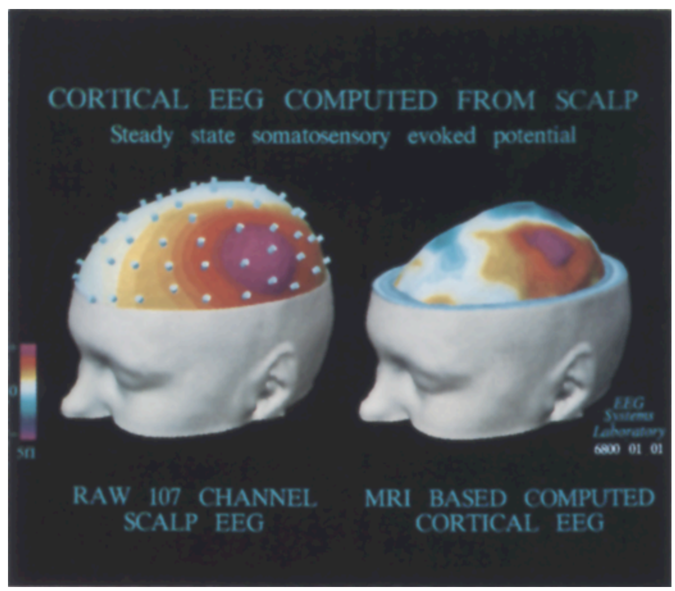

Figure 4. Finite Element Model Deblurring of steady-state somatosensory evoked potentials elicited by 15-Hz stimulation of the left hand of an epileptic patient who had a 64-electrode recording grid implanted for purposes of surgical screening. The single large peak in the potential map (left) is considerably sharpened in the deblurred data (right), which in addition shows some polarity reversals. (All surfaces were reconstructed from horizontal MR images obtained prior to surgery, one of which is shown in part between the scalp and cortex on right.)

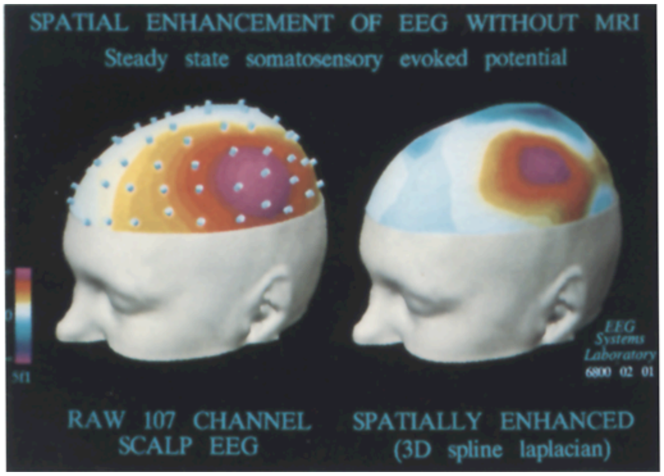

Figure 5. Original scalp potentials (left — same data as figure 4, left) and 3-D spline Laplacian Derivation (right). The Laplacian Derivation also is spatially sharpened compared with the original potential data, but is less detailed than the deblurred data shown in figure 4, right.

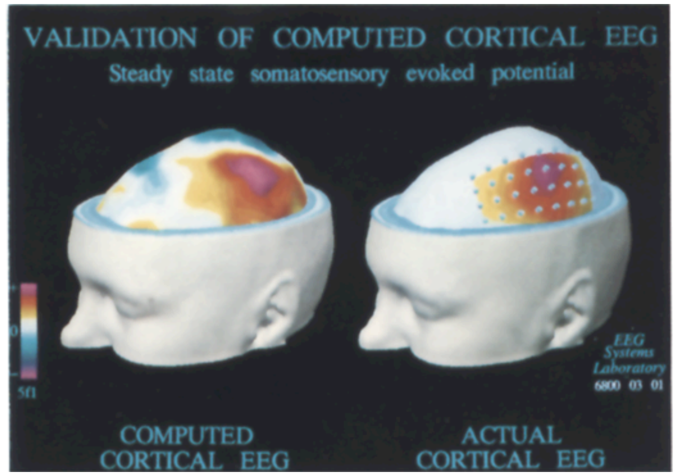

Figure 6. Comparison of deblurred evoked potentials (left — same data as figure 4, right) with the evoked potentials actually recorded from the subdural grid (right) is shown. The area covered by the grid shows a single large peak similar to that in the deblurred data.

Deblurred evoked potentials for the visual stimuli show maxima located near the occipital pole, which is the location of the most likely source, striate cortex (area 17). The auditory deblurred evoked potentials are less clearly localized, as would be expected for this more difficult case and the limited accuracy of our initial FEM model, but are more consistent with bilateral temporal-lobe sources than the raw scalp potentials would indicate.

Equivalent-Dipole Source Localization For Somatic and Visual Stimuli

Single equivalent dipole modeling of the head was performed for each of the three 15 Hz somatosensory

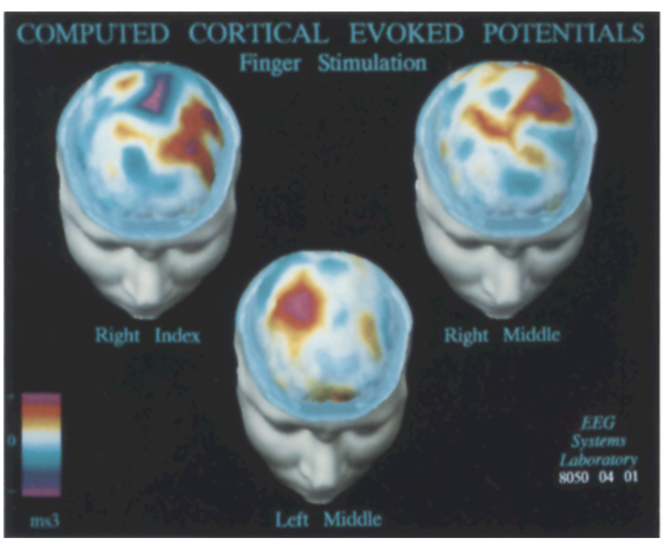

Figure 7. Deblurred steady-state evoked potentials elicited by 15-Hz stimulation of left middle and right middle and index fingers of a normal subject (ms3). All three cases show the expected contralateral maximum in activity, while the response to right index finger stimulation differs markedly from that for the right middle finger.

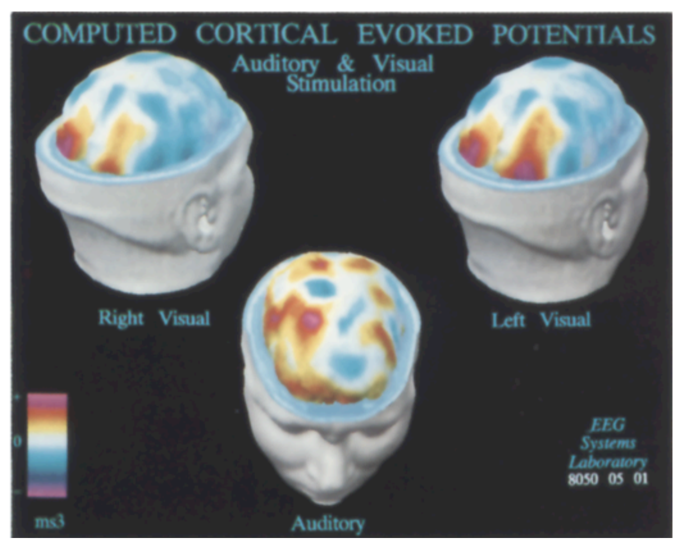

Figure 8. Deblurred steady-state evoked potentials elicited by 15-Hz auditory and visual stimulation. Rear view of the head shows maximal activity at the occipital pole for the parafoveal right and left visual quadrant stimulation. The auditory response is less clear, but is greater over the right hemisphere.

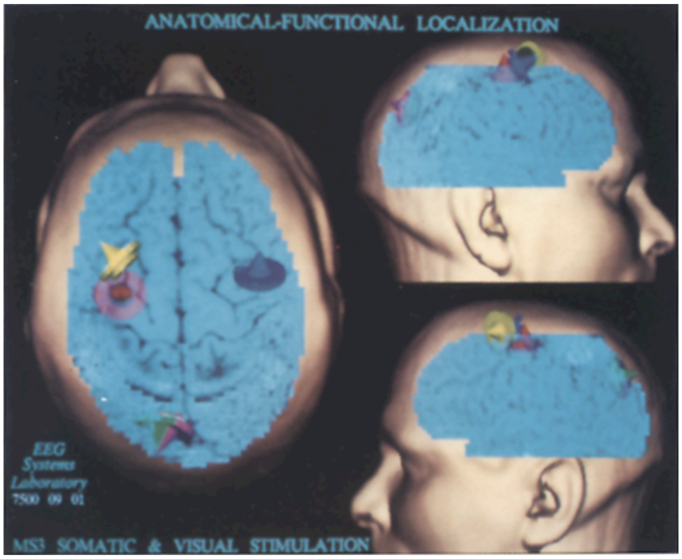

Figure 9. Single equivalent dipole modeling for each of the three 15-Hz somatosensory stimulus conditions shown in figure 7. Dipoles are shown with respect to the scalp surface and a cubic brain model constructed from the subject's MR images. Each dipole is represented as a disk with its center on the dipole's location, and with a cone pointing in the dipole's direction. Dipole color indicates stimulus as follows: left middle finger (blue), right middle (red), and right forefinger (yellow). Each dipole appears in the contralateral hemisphere, and the dipole for the forefinger is located slightly more lateral than that for the middle finger, consistent with the known locations of the somatosensory projection areas.

stimulus conditions shown in figure 7. Figure 9 shows the dipoles with respect to the scalp surface and a cubic brain model constructed from the subject's MRI (see Gevins et al. 1990). Each dipole is represented as a disk with its center on the dipole's location, and with a cone pointing in the dipole's direction. Dipole color indicates stimulus as follows: left middle finger (blue), right middle (red), and right forefinger (yellow). The goodness of fit was 85, 96 and 97% for right forefinger, right middle finger, and left middle finger, respectively. Each dipole appears in the contralateral hemisphere, and the dipole for the forefinger is located slightly more lateral than that for the middle finger, consistent with the known locations of the sensory projection areas and other physiological source localization results (Okada et al. 1984; Wood et al. 1985; Luders et al. 1986). Although dipole models are not physiologically realistic, they are nonetheless useful for locating the center of mass of primary sensory cortex. Although some proponents of MEG technology have maintained otherwise, equivalent dipole modeling performed with EEG appears to be no less accurate than that performed with MEG. This same conclusion has recently been demonstrated via direct comparison of MEG and EEG localization for dipoles generated by stimulation of electrodes implanted in epileptic patients (Cohen et al. 1990).

Conclusion

Although hundreds of millions of dollars have been invested in developing other forms of functional brain imaging including PET, SPECT, MRSI, and MEG, the EEG has been relatively overlooked by the scientific, medical and business community at large. This is unfortunate since it is clear that EEGs, coupled with MRIs, are capable of providing images of superficial cortical electrical activity with very high temporal resolution and spatial detail approaching that of O15 PET scans. EEGs are inherently a low cost technology. They require neither bulky, expensive sensor technologies, nor ionizing radiation. We sincerely hope that EEG will receive the attention and subsequent large-scale development that it merits.

References

Basar, E. (Ed.). Dynamics of Sensory and Cognitive Processing by the Brain. Springer-Verlag, Heidelberg, 1989.

Cohen, D., Cuffin, B.N., Yunokuchi, K., Maniewski, R., Purcell, C., Cosgrove, G.R., Ives, J., Kennedy, J.G. and Schomer, D.L. MEG versus EEG localization test using implanted sources in the human brain. Ann. Neurol., 1990, 28: 811-817.

Duffy F.M. (Ed.). Topographic Mapping of Brain Electrical Activity. Buttersworths, Boston, 1986.

Fender, D.H. Source localization of brain electrical activity. In: A.S. Gevins and A. Remond (Eds.), Handbook of Electroencephalography and Clinical Neurophysiology: Vol.1, Methods of Analysis of Brain Electrical and Magnetic Signals. Elsevier, Amsterdam, 1987: 355-403.

Foley, J.D., van Dam, A., Feiner, S.K. and Hughes, J.F. Computer Graphics: Principles and Practice, 2nd Ed. Addison-Wesley, New York, 1990.

Freeman, W.J. Use of spatial deconvolution to compensate for distortion of EEG by volume conduction. IEEE Trans. Biomed. Engr., 1980, 27: 421-429.

Gevins, A.S. Application of pattern recognition to brain electrical potentials. IEEE Trans. Pattern Ana. Mach. Intell., 1980, 12: 38

Gevins, A. Dynamic functional topography of cognitive tasks. Brain Topography, 1989, 2: 37-56.

Gevins, A.S. Dynamic patterns in multiple lead data. In: J.W. Rohrbaugh, R. Parasuraman and R. Johnson, Jr. (Eds.), Event-Related Brain Potentials: Basic Issues and Applications. Oxford University Press, New York, 1990: 44-56.

Gevins, A.S. and Bressler, S.L. Functional topography of the human brain. In: G. Pfurtscheller and F.H. Lopes da Silva (Eds.), Functional Brain Imaging. Hans Huber Publishers, Bern, 1988: 99-116.

Gevins, A.S. and Morgan, N.H. Applications of neural-network

(NN) signal processing in brain research. IEEE ASSP Trans., 1988, 7: 1152-1161.

Gevins, A.S. and Remond, A. (Eds.). Methods of Analysis of Brain Electrical and Magnetic Signals. Handbook of Electroencephalography and Clinical Neurophysiology, Vol.1. Elsevier, Amsterdam, 1987.

Gevins, A.S., Bressler, S.L., Morgan, N.H., Cutillo, B.A., White, R.M., Greer, D.S. and Illes, J. Event-related covariances during a bimanual visuomotor task. I. Methods and analysis of stimulus- and response-locked data. Electroenceph. Clin. Neurophysiol., 1989, 74: 58-75.

Gevins, A.S., Doyle, J.C., Cutillo, B.A., Schaffer, R.E., Tannehill, R.S., Ghannam, J.H., Gilcrease, V.A. and Yeager, C.L. Electrical potentials in human brain during cognition: New method reveals dynamic patterns of correlation. Science, 1981, 213: 918-922.

Gevins, A., Brickett, P., Costales, B., Le, J., Reutter, B. Beyond topographic mapping: Towards functional-anatomical imaging with 124-channel EEGs and 3-D MRIs. Brain Topography, 1990, 3: 53-64.

Heffernan, P.B. and Robb, R.A. A new method for shaded surface display of biological and medical images. IEEE Trans. Medical Imaging, 1985, 4: 26-38.

Hill, C.D., Kearfott, R.B and Sidman, R.D. The inverse problem of electroencephalography using an imaging technique for simulating cortical surface data. In: R. Vichnevetsky, P. Borne, J. Vignes (Eds)., Proc. 12th IMACS World Cong., Vol. 3, 1988: 735-738.

Hjorth, B. An on-line transformation of EEG scalp potentials into orthogonal source derivations Electroenceph. Clin. Neurophysiol., 1975, 39: 526-530.

Jack, C.R., Marsh, W.R., Hirschorn, K.A., Sharbrough, F.W., Cascino, G.D., Karwoski, R.A. and Robb, R.A. EEG scalp electrode projection onto three-dimensional surface rendered images of the brain. Radiology, 1990, 176: 413-418.

Jasper, H.H. The ten-twenty electrode system of the international federation. Electroenceph. Clin. Neurophysiol., 1958, 10: 371-375.

John, E.R. Neurometrics: Clinical Applications of Quantitative Electrophysiology. Lawrence Erlbaum, Hillsdale, NJ, 1977.

Le, J. and Gevins, A.S. Laplacian derivation of scalp-recorded EEGs computed with realistic head model and 3-D spline. In preparation, a.

Le, J. and Gevins, A.S. MRI-based finite element model deblurring of scalp-recorded EEGs. In preparation, b.

Lehmann, D. Spatial analysis of EEG and evoked potential data. In: F.H. Duffy (Ed.), Topographic Mapping of Brain Electrical Activity. Buttersworths, Boston, 1986: 23-61.

Levin, D.N., Hu, X., Tan, K.K. and Galhotra, S. Surface of the brain: three-dimensional MR images created with volume-rendering. Radiology, 1989, 171: 277-280.

Levoy, M. Display of surfaces from volume data. IEEE Comput. Graph. and Applic., 1988, 8: 29-37.

Lopes da Silva, F.H., Storm van Leeuwen W. and Remond, A. (Eds.). Handbook of Electroencephalography and Clinical Neurophysiology, Vol. 2: Clinical Applications of Computer Analysis of EEG and other Neurophysiological Signals. Elsevier, Amsterdam, 1986.

Lorensen, W. E. and Cline, H. E. Marching cubes: A high resolution 3-D surface construction algorithm. Comput. Graph., 1987, 21: 163-170.

Luders, H., Dinner, D.S., Lesser, R.P. and Morris, H.H. Evoked potentials in cortical localization. J. Clin. Neurophysiol., 1986, 3: 75-84.

Mintun, M.A., Fox, P.T. and Raichle, M. A highly accurate method of localizing regions of neuronal activation in the human brain with positron emission tomography. J. Cereb. Blood Flow Metab. 1989, 9: 96-103.

Nicholas, P. and Deloche, G. Convolution computer processing of the brain electrical image transmission. Int. J. Bio-Med. Comput., 1976, 7: 143-159.

Nunez, P. Estimation of large scale neocortical source activity with EEG surface Laplacians. Brain Topography, 1989, 2: 141-154.

Okada, Y.C., Tannenbaum, R., Williamson, S.J. and Kaufman, L. Somatopic organization of the human somatosensory cortex revealed by neuromagnetic measurement. Exp. Brain Res. 1984, 56: 197-205.

Pfurtscheller, G. and Lopes da Silva, F.H. (Eds.). Functional Brain Imaging. Hans Huber Publishers, Bern, 1988.

Reutter, B.W. and Gevins, A.S. Algorithms for analysis of Magnetic Resonance Images. In preparation.

Sidman, R.D., Kearfort, R.B., Major, D.J., Hill, D.C., Ford, M.R., Smith, D.B., Lee, L. and Kramer, R. Development and application of mathematical techniques for the noninvasive localization of the sources of scalp-recorded electric potentials. In: J. Eisenfield and D.S. Levine (Eds.), IMACS Trans. Scientific Computing., Vol. 5. J. C. Baltzer AG, Basel, 1989: 133-157.

Wang, J., Cohen, L.M. and Hallett, M. Scalp topography of somatosensory evoked potentials following electrical stimulation of femoral nerve. Electroenceph. Clin. Neurophysiol., 1989, 74: 112- 123.

Wood, C.C., Cohen, D., Cuffin, B.N., Yarita, M. and Allison, T. Electrical sources in human somatosensory cortex: Identification by combined magnetic and potential recordings. Science, 1985, 227: 1051-1053.